AIAA 81-0022R

A New Technique for Multirate Digital Control Design and Sample Rate Selection

Douglas P. Glasson*
The Analytic Sciences Corporation, Reading, Mass.

A new approach for designing multirate digital flight control systems based on optimal control theory is described. The error rejection properties of control systems designed by the new technique are investigated through a case study. The example considered is the F-14 aircraft controlled by a multirate proportional-plus-integral controller. The aircraft/controller system is "flown" through a turbulent atmosphere; a covariance analysis of state variable errors determines the ability of the controller to reject turbulence-induced errors. The controller sample rate and control sequence are varied to determine their influence on the disturbance rejection properties of the controller. Finally, a sample rate optimization scheme based on performance/computation tradeoff is presented.

I. Introduction

THE practical need for multiple sample rate flight control systems is a consequence of the finite computing capabilities of onboard digital computers and the multiple information rates of onboard instruments. Although digital computer technology continues to advance significantly, new and expanded software requirements for such functions as navigation, display, and control manage to keep pace with improvements in computational capability. Accordingly, the flight control system designer is always allocated a fixed (and usually limiting) amount of computational capability to implement a control design. In modern flight control system applications, the problem of implementing a desired algorithm within a limited computational capability is compounded by a need to accommodate high-frequency effects such as vehicle flexibility. Functions associated with bending effects (i.e., instrument output filtering or active structural control) may demand sample rates an order of magnitude higher than is necessary for suitable control of rigid body modes of vehicle motion. Faced with widely varying sample rate requirements among the dynamic modes of the vehicle; a multirate control structure is the solution to computational limitations and multiple information rates.

Synthesizing a multirate control system to meet desired specifications has been a difficult task. Ad hoc approaches have typically been used in which a suitable analog design is converted to a digital design via Tustin transform techniques. In this case multirate designs are generated by a trial-and-error process of running the low bandwidth compensating elements at low sample rates and evaluating the resulting system performance via simulation. Classically based techniques for multirate system analysis are available[1-3]; however, these techniques are limited in application due to the significant growth of dimensionality that they entail. Such techniques are also analysis, as opposed to synthesis, approaches; hence creating a control design is still an iterative procedure. In the present paper, a new multirate design technique[4,5] based on optimal control is described which obviates dimensionality problems characteristic of classical techniques. In addition, this technique offers a systematic method for converting a desired analog control design to an equivalent multirate digital design without approximation.

Presented as Paper 81-0022 at the AIAA 19th Aerospace Sciences Meeting, St. Louis, Mo., Jan. 12-15, 1981; submitted March 2, 1981; revision received March 8, 1982.

*Project Leader. Member AIAA.

The very important issue of relative stability, or robustness, of the system may not be addressed if one designs only to specifications related to deterministic response characteristics. Robustness is quantified by many methods (e.g., phase/gain margins, disturbance rejection bandwidth) but generally represents some measure of the system's ability to resist disturbances and tolerate design uncertainties. Robustness is a very real concern in flight control applications. The designer never has exact knowledge of the vehicle aerodynamics or the flight conditions; accordingly, the flight control system must be designed to tolerate uncertainties, remain stable, and perform within a specified range of handling qualities.

The new multirate design procedure and the transient response characteristics of systems designed by this procedure are described in detail in Refs. 4 and 5; hence they will only be summarized in the present discussion. Disturbance rejection properties and performance/computation optimization of multirate control systems are the primary topics of the present paper.

II. Summary of the Design Procedure

It is assumed that the plant (vehicle) dynamics to be controlled are described by the linear-time-invariant differential equation:

$$\dot{x}(t) = Fx(t) + Gu(t) \tag{1}$$

where x is the state vector and u is the control vector. The control u is to be sampled and held at time instants t_k, with all elements of u possibly sampled at different rates.

The discrete-time dynamics of the continuous plant are described by

$$x_{k+1} = \phi x_k + \Gamma_f u_{f_k} + \Gamma_s u_{s_k} \tag{2}$$

where

$$\phi = e^{FT_s} \qquad \Gamma = \int_0^{T_s} e^{F\tau} G \mathrm{d}\tau$$

and the control vector, u, has been partitioned into subsets u_f and u_s to signify those controls computed at the base rate and those scheduled at lower rates, respectively.

Development of the multirate regulator structure requires augmentation of the natural plant dynamics with holding circuit states (i.e., holding the slow controls between updates); the discrete-time dynamics of this augmented system (for the

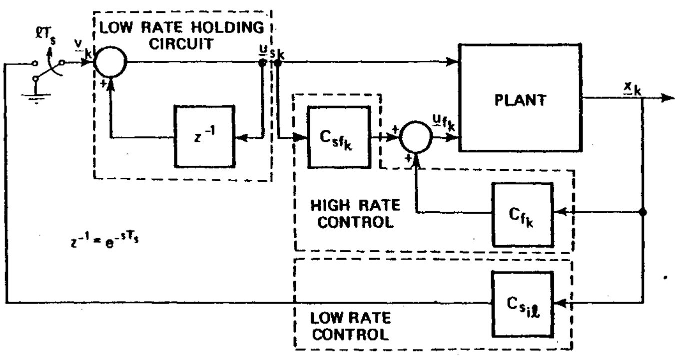

Fig. 1 Multirate regulator structure.

case of two sample rates) are given by

$$\begin{bmatrix} x_{k+1} \\ u_{s_{k+1}} \end{bmatrix} = \begin{bmatrix} \phi & \Gamma_s \\ 0 & I \end{bmatrix} \begin{bmatrix} x_k \\ u_{s_k} \end{bmatrix} + \begin{bmatrix} \Gamma_f & \Gamma_s \delta_{k,il} \\ 0 & I\delta_{k,il} \end{bmatrix} \begin{bmatrix} u_{f_k} \\ v_k \end{bmatrix} \tag{3}$$

where $\delta_{k,il}$ is the Kronecker delta function.

The structure of a multirate optimal regulator for the case of two sample rates is shown in Fig. 1. As the block diagram indicates, one control channel, u_f, is updated at a fast rate, T_s^{-1} samples per second; u_s is computed at a slower rate, $(lT_s)^{-1}$ samples per second, and is held between computations by a holding circuit. Recomputation of u_s is accomplished by adding an increment, v_k, to the holding circuit on cycles when $k=il$; on all other cycles v_k is set to zero. Another result of the present design procedure is that the slow control is crossfed to the fast control channel on cycles between slow control updates.

The periodic gains—C_{f_k}, $C_{s_{il}}$, and C_{sf_k}—are obtained by propagating the optimal regulator Ricatti equation from infinity backwards to (periodic) steady state. The derived periodic regulator gains are

$$C_k = \begin{bmatrix} C_{f_{il}} & C_{sf_{il}} \\ & C_{s_{il}} \end{bmatrix} \qquad k=il$$

$$C_k = [C_{f_k} C_{sf_k}] \qquad k \neq il \tag{4}$$

Note that the dimensions of C_k change according to the number of controls that are computed on cycle k.

The closed-loop dynamics of the multirate system are determined by the choice of the quadratic cost functional weighting matrices used in the optimal regulator problem, i.e., with the following definition of the cost functional:

$$J = \frac{1}{2} \sum_{k=0}^{\infty} \left\{ (x_k^T \; u_{s_k}^T) \hat{Q}_k \begin{pmatrix} x_k \\ u_s \end{pmatrix} + 2(x_k^T \; u_{s_k}^T) \hat{M}_k \tilde{u}_k + \tilde{u}_k^T \hat{R}_k \tilde{u}_k \right\} \tag{5}$$

The choice of the matrices $\hat{Q}_k$, $\hat{M}_k$, and $\hat{R}_k$ ultimately determines the dynamics of the closed-loop system. A procedure is described in Ref. 4 for deriving the $\hat{Q}_k$, $\hat{M}_k$, and $\hat{R}_k$ matrices from the weighting matrices of a specified continuous-time regulator design [for the continuous plant dynamics given by Eq. (1)]. This procedure is summarized here.

1) A *continuous-time* regulator is designed to meet continuous-time performance specifications.

2) Discrete-time regulator weighting matrices for the single-rate case are derived from those used to design the continuous-time regulator.

3) The discrete-time periodic weighting matrices used to solve for the multirate gains are constructed from the single-rate matrices. The multirate gains are derived from the periodic steady-state solution of the discrete-time Ricatti equation.

The first step involves the normal iterative design process associated with designing an optimal regulator; i.e., trial-and-error assignment of weighting matrix elements to yield a regulator that meets the design specifications. The relationships presented in Ref. 6 are then used to compute the single-rate (i.e., fast rate) discrete-time weighting matrices from the continuous-time matrices. Using the augmented system representation, Eq. (3), and the relationships in Ref. 6, expressions are derived for the multirate weighting matrices; inspection of these expressions indicates that the multirate matrices can be constructed from the single-rate matrices computed in step 2 above. An implicit benefit of this three-step approach is that the deterministic performance of the continuous-time, single-rate discrete-time, and multirate discrete-time controllers can be compared on a one-to-one basis; i.e., each control design is based on optimizing the same continuous-time cost functional.[6]

Extension of the two-sample-rate control structure described here to the multirate case (i.e., more than two sample rates) is straightforward. Consider organizing the plant inputs into two groups: those computed at the fastest rate, u_f, and those scheduled at lower rates, u_s. Again augmenting the plant dynamics with slow control holding circuits (which now are operating at multiple rates) the discrete-time dynamics of the augmented system are given by

$$\begin{bmatrix} x_{k+1} \\ u_{s_{k+1}} \end{bmatrix} = \begin{bmatrix} \Phi & \Gamma_s \\ 0 & I \end{bmatrix} \begin{bmatrix} x_k \\ u_{s_k} \end{bmatrix} = \begin{bmatrix} \Gamma_f & \Gamma_s \Delta_k \\ 0 & I\Delta_k \end{bmatrix} \begin{bmatrix} u_{f_k} \\ v_k \end{bmatrix} \tag{6}$$

where

$$\Delta_k = \begin{bmatrix} \delta_{k,i_1 l_1} & 0 & \cdots & & 0 \\ 0 & \delta_{k,i_2 l_2} & & & \vdots \\ \vdots & & & & \vdots \\ \vdots & 0 & & & 0 \\ 0 \; \cdots & 0 & 0 & & \delta_{k,i_{m'} l_{m'}} \end{bmatrix} \tag{7}$$

where m' is the dimension of v and

$$\delta_{k,i_j l_j} = \begin{cases} 1 & (i_j l_j = k) \\ 0 & (i_j l_j \neq k) \end{cases} \tag{8}$$

The matrix Δ_k is a generalization of the Kronecker delta functions used in the two-sample-rate case. Each diagonal element of Δ_k nulls the input to a particular low rate control holding circuit on cycles between new computations of that control. For example, if u_{s2} is computed every two cycles (i.e., $l_2 = 2$) then the second diagonal element of Δ_k will be zero on cycles when k is not a multiple of 2 (i.e., $k \neq i_2 l_2$).

III. Disturbance Rejection Properties

The design approach described in Sec. II of this paper is a procedure for achieving desired transient response charac-

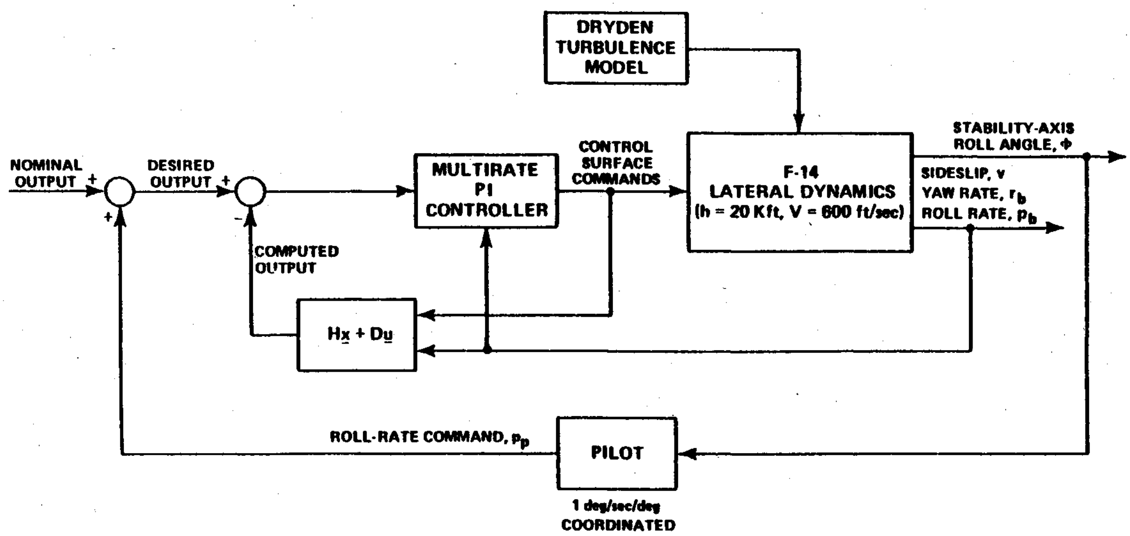

Fig. 2 Example multirate system.

teristics (i.e., response time, overshoot) from a multirate system. In this section the disturbance rejection properties of multirate control systems designed by the present technique are considered. As described in Sec. II, the three-step procedure used in the present design approach results in equivalent deterministic performance of the multirate system and a specified continuous-time system (i.e., the same quadratic cost functional is minimized by both systems). With this equivalence of deterministic performance, the effect of variations in control computation rate on error rejection properties can be studied as an independent influence.

Consider the system described by Eq. (2) disturbed by an uncorrelated Gaussian random process:

$$x_{k+l} = \phi x_k + \Gamma_f u_{f_k} + \Gamma_s u_{s_k} + w_k \qquad (9)$$

with

$$E(w_i) = 0 \qquad (10)$$

$$E(w_i w_j^T) = Q\delta_{ij} \qquad (11)$$

Note that the system description given by Eq. (9) covers the case of a correlated disturbance process (such as atmospheric turbulence); in that case, the state vector x includes the state of the disturbance process, and the transition matrix includes the dynamics of the correlated disturbance process.

The dynamics of the closed-loop multirate system are given by

$$\tilde{x}_{k+l} = \bar{\phi}_k \tilde{x}_k + \tilde{w}_k \qquad (12)$$

where

$$\tilde{x}_k^T = (x_k^T \;\; u_{sk}^T) \qquad (13)$$

$$\tilde{w}_k^T = (w_k^T \;\; 0) \qquad (14)$$

$$\bar{\phi}_k = \begin{bmatrix} \phi & \Gamma_s \\ 0 & I \end{bmatrix} - \begin{bmatrix} \Gamma_f & \Gamma_s \Delta_k \\ 0 & I\Delta_k \end{bmatrix} \begin{bmatrix} C_{f_k} & C_{sf_k} \\ & C_{sk} \end{bmatrix} \qquad (15)$$

The covariance dynamics of the system described by Eq. (12) are

$$P_{k+l} = \bar{\phi}_k P_k \bar{\phi}_k^T + \tilde{Q} \qquad (16)$$

with

$$P = E(\tilde{x}_k \tilde{x}_k^T) \qquad (17)$$

$$\tilde{Q} = E(\tilde{w}_k \tilde{w}_k^T) \qquad (18)$$

In steady state, the solution of Eq. (16) is periodically time-varying with a period equal to the number of cycles over which the control computation schedule repeats itself; i.e.,

$$P_{k+l} = P_k \qquad (19)$$

Propagating Eq. (16) over l cycles and using Eq. (19), one obtains

$$P_k = \phi^* P_k \phi^{*T} + Q^* \qquad (20)$$

where

$$\phi^* = \bar{\phi}_{k+l-1} \bar{\phi}_{k+l-2} \cdots \phi_k \qquad (21)$$

$$Q^* = \sum_{i=k+l}^{k+l-1} \phi_i^* \tilde{Q} \phi_i^{*T} + \tilde{Q} \qquad (22)$$

$$\phi_i^* = \bar{\phi}_{k+l-1} \bar{\phi}_{k+l-2} \cdots \bar{\phi}_i \qquad (23)$$

To determine the periodic steady-state solution to Eq. (16), the full-period covariance equation, Eq. (20), is solved. Then the remaining values of P_k over the complete control cycle are determined by propagating Eq. (16) for $l-1$ cycles.

IV. Example System Description

An example system, analyzed to evaluate the disturbance rejection properties of a typical multirate system designed by the present technique, is described in this section. Figure 2 is a block diagram of the example system. The system is comprised of the linearized lateral dynamics of the F-14 in trimmed level flight (at an airspeed of 600 ft/s at 20,000 ft), Markov models of turbulence[7] (sideslip, yaw rate, and roll rate components at the specified flight condition), a coordinated pilot (attitude feedback) model, and a multirate proportional-plus-integral control system designed by the present technique. The controls in this case are differential stabilator and rudder.

The eigenvalues of the continuous-time vehicle/control system used to develop the multirate system are summarized in Table 1. Again, the present design technique yields a multirate closed-loop system with deterministic dynamics (i.e., transient response characteristics) very similar to those of the continuous-time system. Subsequent analysis si concerned with the stochastic error rejection properties of the multirate system as a function of control sample rates.

Table 1 Continuous-time closed-loop eigenvalues

Dynamic mode	Natural frequency, rad/s	Damping ratio	Time constant, s
Roll command	4.32	0.675	...
Dutch roll	3.54	0.714	...
Lateral control	...	...	1.64
Sideslip command	...	...	1.19

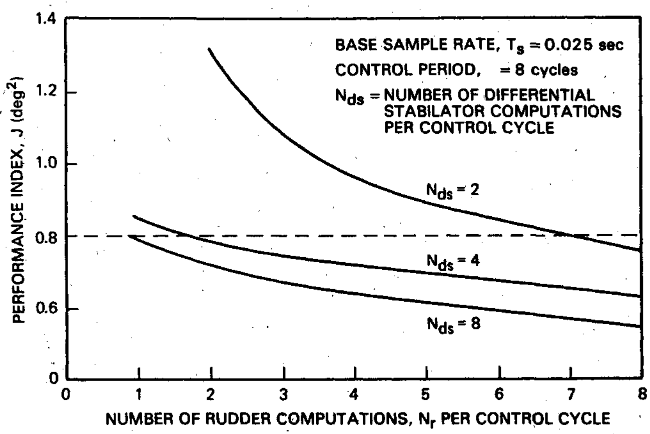

Fig. 3 Performance of multirate system as a function of control sequence.

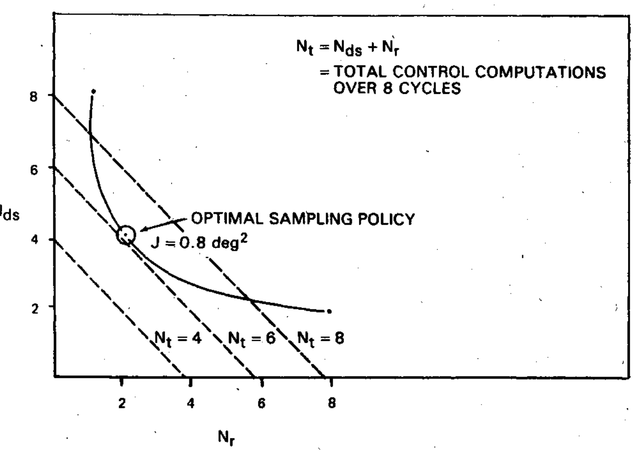

Fig. 4 Sampling policy optimization for a fixed level of performance.

The covariance analysis formulation outlined above was applied to the plant/disturbance/controller system described in Fig. 2; the results of the analysis are given in this section. The control computation rate and schedule of the controller are varied to determine their effect on the disturbance rejection properties of the system.

The performance index for the control system is the sum of the stability-axis roll angle and sideslip angle covariances; i.e.,

$$J = P_{44} + P_{11}/V^2 \tag{24}$$

This choice of performance index gives equal weighting to deviations from wings-level flight and undesired sideslipping (with attendant lateral acceleration). In the example considered here, periodicity of the covariance equation solution was observed. The variations of the variances of interest were in the fourth significant figure; for this case, a figure of merit based on average values of P_{11} and P_{44} is adequate.

The results of the covariance analysis/figure-of-merit computation for a matrix of differential stabilator-rudder schedules is presented in Fig. 3. Here the base sample rate is 40 Hz (T_s = 0.025 s) and the control period is 8 cycles (0.2 s). As shown in the figure, the three curves indicate the performance of the system for three rates of differential stabilator computation (i.e., the number of differential stabilator computations every 8 cycles) as a function of rudder computation rate. In all cases, reducing the number of rudder computations performed during the 8-cycle period increases the performance index; this is primarily due to the increase in sideslip covariance as the rudder rate is reduced. Similarly, as the number of differential stabilator computations is reduced, the covariance of roll angle error increases, thereby increasing the performance index.

A potential tradeoff of performance and computational load can be identified at this point. Suppose that it is desired that the performance index has a value of 0.8 deg² or less (indicated by the dotted line in Fig. 3). The cross-plot of J=0.8 deg² into an N_{ds}/N_r axis system is shown in Fig. 4. Since each differential stabilator or rudder control computation "costs" the same (i.e., each involves the same number of multiplications and additions per computation) curves of constant computational burden can be represented by the dashed straight lines plotted in Fig. 4. The tangent intersection of the N_t=6 line with the J=0.8-deg² curve indicates that the desired performance can be achieved with the minimum number of computations if the control schedule includes four differential stabilators and two rudder computations per 8-cycle period.

V. Conclusions

In this paper a methodology for evaluating the disturbance rejection properties of a multirate system is presented. This methodology is based on steady-state covariance analysis of the multirate system with variations of control schedule to determine disturbance rejection sensitivity to control computation rates.

The control error covariance of a multirate system is periodic in steady state with a period equal to the control schedule period. The periodic history of the steady-state covariance solution is obtained by constructing and solving a Liapunov equation which represents the full control period covariance dynamics, then propagating the cycle-to-cycle covariance equation over the control period.

The disturbance rejection properties of an example multirate system are evaluated as a function of control scheduling. As expected, the disturbance rejection performance of the example system degrades with lower sample rates of the controls. An approach for optimization of the performance/computation tradeoff is presented.

References

[1] Whitbeck, R.F. and Hofmann, L.G., "Analysis of Digital Flight Control Systems with Flying Qualities Application," Vol. 2, Rept. AFFDL-TR-78-115, Air Force Flight Dynamics Laboratory, Wright-Patterson Air Force Base, Ohio, Sept. 1978.

[2] Konar, A.F. and Lee, J.F., "Analysis of Multiloop, Multirate Digital Control Systems," 1976 IEEE Conference on Decision and Control, Clearwater, Fla., Dec. 1976.

[3] Saxe, R., "DIGIKON: The Direct Digital Control System Analysis Program for Shuttle," 1976 IEEE Conference on Decision and Control, Clearwater, Fla., Dec. 1976.

[4] Glasson, D.P., "Research in Multirate Estimation and Control," The Analytic Sciences Corporation, Technical Report, TR-1356-1, Dec. 1980.

[5] Broussard, J.R. and Glasson, D.P., "Optimal Multirate Flight Control Design," *Proceedings of the 1980 Joint Automatic Control Conference*, San Francisco, Calif., Aug. 1980, pp. WPI-E.

[6] Gran, R., Berman, H., and Rossi, M., "Optimal Digital Flight Control for Advanced Fighter Aircraft," *Journal of Aircraft*, Vol. 14, Jan. 1977, pp. 32-37.

[7] Anon., "Flying Qualities of Piloted Airplanes," Military Specification No. MIL-F-8785B (ASG), 7 Aug. 1969, pp. 47-52.